VOL. 11, NO. 20, OCTOBER 2016 ISSN 1819-6608
ARPN Journal of Engineering and Applied Sciences

www.arpnjournals.com

CFD SIMULATION OF BUBBLING FLUIDIZED BED: EFFECT OF DISTRIBUTOR PLATE ORIFICE PATTERN CONFIGURATION ON HYDRODYNAMICS OF GAS-SOLID MIXING

Iman Eslami Afrooz[1], Chandra Mohan Sinnathambi[2], Saravanan Karuppanan[1] and Dennis Ling Chuan Ching[2]
[1]Department of Mechanical Engineering, Universiti Teknologi Petronas, Seri Iskandar, Perak, Malaysia
[2]Department of Fundamental and Applied Sciences, Universiti Teknologi Petronas, Seri Iskandar, Perak, Malaysia
E-Mail: imaneslami@hotmail.com

ABSTRACT

The gas-solid mixing pattern in a fluidized bed is significantly affected by distributor plates. In order to study this impact, two different distributer plates orifice arrangement, namely, triangular and radial (TDP and RDP) are designed. The solid circulation patterns caused by each orifice arrangements are then predicted numerically. To this end, Eulerian-Eulerian (EE) approach through Computational Fluid Dynamic (CFD) is utilized. As a final point, the simulated particle volume fraction, particle velocity and bed pressure drop are compared. It was found that the distribution of solid volume fraction is more homogeneous while TDP was used. The regular pattern of radial particle velocity was also found for TDP. These indicate that particle motion mainly concentrates in the region between the core and the wall of the bed. However, chaotic solid motion at the core region was observed for RDP.

Keywords: CFD, bubbling fluidized bed, fluidization, hydrodynamic.

INTRODUCTION

The first demonstration of fluidization was introduced by Fritz Winkler in 1921 [1]. Since then fluidization is found in many operations in petro-chemical processing, mineral processing, chemical, pharmaceutical, electronic, and power-generation industries. Studying the hydrodynamics of fluidization is necessary for the design of fluidized bed reactors. This study can be done through the experiment and simulation works. The experimental study is costly and time-consuming due to the construction and testing of various models. However, the use of a reliable numerical technique reduces these extra costs significantly. Accurate numerical algorithms give us a powerful tool to accurately predict the hydrodynamics behavior of multiphase flows having complex geometries. Furthermore, the variety of shapes and models can be easily designed and tested numerically followed by a limited number of experiments for comparison and validation purpose.

Thanks to the development of computers and computational techniques, the complex governing equations such as Navier-Stokes equations used in single-phase fluid mechanics and conservative equations in gas-solid flow, have been solved numerically. These equations were originally developed by Jackson, Soo, Garg and Pritchett [2-4]. One of the first numerical analysis of solid flow in fluidized bed was done by Arastoopour and Gidaspow [5]. Gidaspow [6] predicted the formation, growth, and the bursting of bubbles in 1983. Ettehadieh *et al*. [7] predicted the velocity profiles of jets which were in good agreement with experimental measurements. Gidspow [8] modeled conservative equations for gas solid flow. Numerical methods have been developed for two-phase flows by using Computational Fluid Dynamic (CFD) to compute erosion rates in fluidized bed tubes [9]. Since then CFD has received more and more attention because of its ability in simulating the complex multiphase flows.

The major concern in fluidization bed systems is to achieve good gas-solid mixing and to prevent agglomeration of the particles which can cause rapid defluidization of the entire bed. The good mixing of gas-solid cannot be reached except by using proper distributor plate orifice arrangement. This shows the importance of distributor plate design in designing the fluidized beds.

In this study, the Eulerian-Eulerian two-fluid model in combination with kinetic theory of granular flow (KTGF) is utilized to study the effect of the orifice pattern on the hydrodynamics of lab-scaled cold flow model (LCM). The LCM is the scaled down version of the existing pilot plant gasifier [10]. Distributor plates used in this study are perforated plates with two different holes' patterns, namely: triangular and radial pitch.

SIMULATION APROACH

The simulation set up used in this study is shown in Figure-1. The computational domain is a cylinder with the bed diameter of 0.0762 m and height of 1 m. Pressure outlet boundary condition was employed at the top of the riser and the velocity inlet boundary condition was imposed at the bottom of the bed.

Table-1 shows the simulation condition details used in this research. Sand with the density of 2608 kg/m^3 and diameter of 500 μm is considered as bed material which is fluidized with air at ambient conditions. The superficial velocity of 0.46 m/s which is two times of the minimum fluidization velocity was chosen in this study. The static bed height is 0.1 m with solid volume fraction of 0.56.

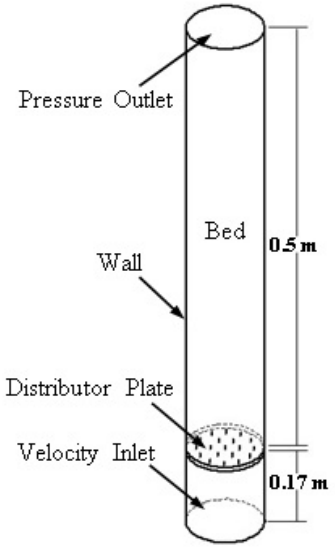

Figure-1. Schematic view of LCM.

Table-1. Details of simulation setup.

Bed diameter	(mm)	76.2
Orifice diameter, d_{or}	(mm)	1
Gas density, ρ_g	(kg/m3)	1.225
Gas viscosity, μ	($\times 10^{-5}$ kg/ms)	1.79
Particle density, ρ_p	(kg/m^3)	2608
Particle diameter, d_p	(μm)	500
Superficial velocity, U	(m/s)	0.46

As shown in Figure-2, two different distributor plates pattern, triangular distributor plate (TDP) and radial distributor plate (RDP), were considered in this study. Simulation were performed in a 3D fashion having a total of 493413 cells. No slip and slip boundary conditions are applied for gas and solid phases, respectively. Since the lower value of specularity coefficient predicts the behavior of gas-solid mixing near the wall more precisely, the value of 0.1 was chosen [11, 12, 13]. The drag model proposed by Syamlal O'Brien was modeled in current simulation. This is the most reliable drag model for the large particles size of 500 μm [12 and 13]. Moreover, the Syamlal O'Brien and the Lun *et al*. viscosity modules were chosen for granular viscosity and solid granular bulk viscosity, respectively.

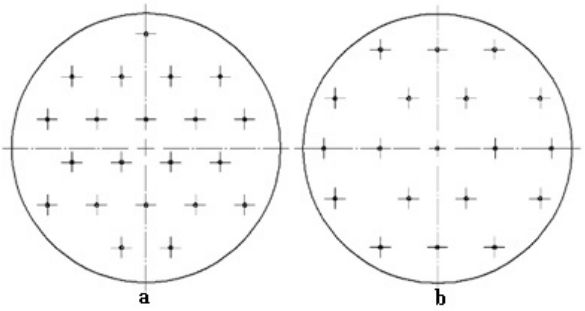

Figure-2. Design of different distributor plates pattern, a. triangular pitch b. radial pitch.

GOVERNING EQUATIONS

The EE Two-Fluid Model (TFM) was utilized to study the hydrodynamic of gas-solid flow in fluidized bed based on the conservation equations of mass and momentum. Since there is no mass transfer, the conservation equation of mass for gas (g) and solid (s) phases can be reduced to

$$\frac{\partial}{\partial_t}\left(\varepsilon_g \rho_g\right) + \nabla.\left(\varepsilon_g \rho_g \vec{v_g}\right) = 0 \quad (1)$$

$$\frac{\partial}{\partial_t}\left(\varepsilon_s \rho_s\right) + \nabla.\left(\varepsilon_s \rho_s \vec{v_s}\right) = 0 \quad (2)$$

where ε, ρ and $\vec{v_s}$ are the volume fraction, density and local velocity, respectively.

The conservation equation of momentum for gas and solid phases are given by

$$\frac{\partial}{\partial_t}\left(\varepsilon_g \rho_g \vec{v_g}\right) + \nabla.\left(\varepsilon_g \rho_g \vec{v_g}\vec{v_g}\right) = -\varepsilon_g \nabla p + \nabla.\bar{\bar{\tau}}_g + \varepsilon_g \rho_g g + K_{gs}\left(\vec{v_s} - \vec{v_g}\right) \quad (3)$$

$$\frac{\partial}{\partial_t}\left(\varepsilon_s \rho_s \vec{v_s}\right) + \nabla.\left(\varepsilon_s \rho_s \vec{v_s}\vec{v_s}\right) = -\varepsilon_s \nabla p - \nabla p_s + \nabla.\bar{\bar{\tau}}_s + \varepsilon_s \rho_s g + K_{gs}\left(\vec{v_g} - \vec{v_s}\right) \quad (4)$$

where K_{gs} is the gas-solid momentum exchange coefficient, p is gas phase static pressure, p_s is solid pressure and g and $\bar{\bar{\tau}}$ are the gravitational acceleration and stress tensor, respectively.

The kinetic theory of granular flow is a widely-used continuum approach in calculating the solid phase properties. In this approach, the solid particle velocity and distribution is represented by the granular temperature model which is proportional to the kinetic energy of the particles' random motion. Therefore, the solid phase properties such as solid viscosity, stress and pressure are a function of a granular temperature. To this end, partial differential equation model is applied to solve the granular temperature model as follows:

$$\frac{3}{2}\left[\frac{\partial}{\partial_t}\left(\varepsilon_s\rho_s\theta_s\right)+\nabla.\left(\varepsilon_s\rho_s\vec{v_s}\theta_s\right)\right]=\left(-\rho_s\bar{I}+\bar{\bar{\tau}}_s\right):\nabla.\vec{v_s}+ \quad (5)$$
$$\nabla.\left(K_{\theta_s}\nabla\theta_s\right)-\gamma\theta_s+\varphi_{gs}$$

where $\left(-\rho_s\bar{I}+\bar{\bar{\tau}}_s\right):\nabla.\vec{v_s}$ is the generation of energy by the solid tensor, $\left(K_{\theta_s}\nabla\theta_s\right)$ is the diffusion of energy while the term K_{θ_s} is the diffusion coefficient, $\gamma\theta_s$ is the collisional dissipation of energy, and φ_{gs} is the energy change between the gas or solid and solid phases.

The diffusion coefficient, K_{θ_s}, is calculated using Syamlal *et al*. model [14] as given below:

$$K_{\theta_s}=\frac{15d_s\varepsilon_s\rho_s\sqrt{\theta_s\pi}}{4(41-33\eta)}\times \quad (6)$$
$$\left[1+\frac{12}{5}\eta^2(4\eta-3)\varepsilon_s g_0+\frac{16}{15\pi}(41-33\eta)\eta\varepsilon_s g_0\right]$$

where $\eta=\frac{1}{2}(1+e_{ss})\cdot$

The collision dissipation of energy, $\gamma\theta_s$, represented by Lun *et al.* [15] and the exchange of fluctuating energy between phases, φ_{gs} are shown in equations 7 and 8, respectively.

$$\gamma\theta_s=\frac{12(1-e_{ee}^{\ 2})g_0}{d_s\sqrt{\pi}}\rho_s\varepsilon_s^{\ 2}\theta_s^{\frac{3}{2}} \quad (7)$$

$$\varphi_{gs}=-3K_{gs}\theta_s \quad (8)$$

In a fluidized bed, the kinetic energy and the interaction of the particles cause the solid pressure and it is increased due to the increase in particle collisions. Since Lun *et al.* solid pressure model [15] is comprised of kinetic and particle collision terms, this model is used for the present simulation as given below:

$$P_s=\varepsilon_s\rho_s\theta_s+2\rho_s(1+e_{ss})\varepsilon_s^{\ 2}g_0\theta_s \quad (9)$$

The above governing equations were solved by using CFD Fluent 15 to predict the bed hydrodynamics of bubbling fluidized beds having Geldart B particles. For this purpose, the Phase Coupled SIMPLE scheme which is an extension of the SIMPLE algorithm [16] to multiphase flows was used to consider the pressure–velocity coupling. Moreover, the Green-Gauss Node Based theorem was used to compute the gradient at the center of the cells. The QUICK and Second Order Upwind discretization schemes were used for the volume fraction and momentum terms. The simulations were performed for 3000 number of time steps with the time step size of 0.001 s.

RESULTS AND DISCUSION

The contour plot of solid volume fraction of bubbling fluidized beds having triangular and radial distributor plates orifice arrangement are shown in Figures-3 and 4, respectively.

The contour plot of solid volume fraction of bubbling fluidized beds having triangular and radial distributor plates orifice arrangement are shown in Figures-3 and 4, respectively.

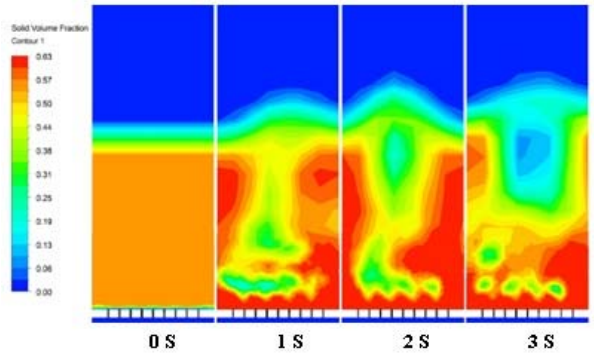

Figure-3. Simulated maps of volume fraction distributions of TDP.

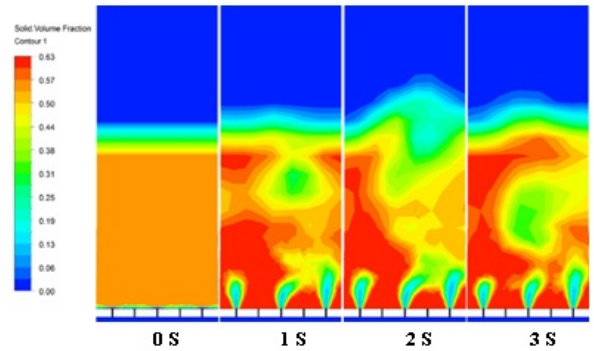

Figure-4. Simulated maps of volume fraction distributions of RDP.

As can be seen in the figures, both distributor plates result in almost the same bed expansion which is a results of bubble formation and movement. Bubbles start to form at a certain height above the distributor plate and they grow while rising to the bed surface due to the coalescence. Considering Figure-3, it is apparent that the air is uniformly distributed throughout the bed which leads to homogeneous distribution of solid volume fraction. It shows a low solid volume fraction in the annular region while the regions near to the walls are experiencing high concentration of solids. This indicates that the concentration of the bubbles is more at the center of the bed. However, the different trend can be seen for RDP (Figure-4). It indicates that bubbles are mostly formed at the annular region rather than the center of the bed.

Figure-5 shows particle concentration at central line and in the axial direction for both cases. In general, particle volume fraction of TDP is reduced with increasing height. It shows the maximum concentration of particles at the surface of the distributor plate. However, zero value can be observed for solid volume fraction of RDP in that

region. This could be due to the direct impact of the gas jet of the central hole of the radial distributor plate. At plotted in the figure, the overall bed height predicted for both cases are almost similar. The intersection points indicate that the predicted volume fraction is same for both distributor plates at the heights of 0.024, 0.071 and 0.13 m.

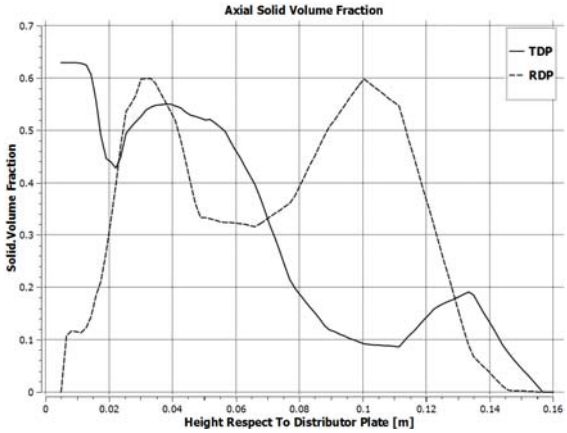

Figure-5. Comparison of axial particle volume fraction at t = 3s for both cases.

Figure-6 shows distributions of solid velocity pattern for both cases at time frame of 3 second. Particle velocity pattern for TDP shows symmetry in the flow pattern. Bubbles are carrying the particles inside their wakes upwards at the center of the bed. Particles then sink downward next to the walls. A rotating circulation of the solid motion is also observed in three different heights for TDP system. This results in lateral solid motion in the top, core and near inlet regions of the bed. These indicate a homogenous mixing of particles while using TDP.

In contrast, nonuniform solid circulation pattern is observed for RDP. Particles go up in the center of the bed and fall down close to the next wall.

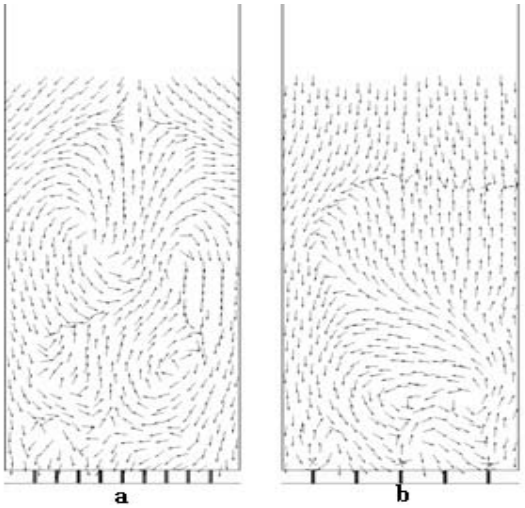

Figure-6. Comparison of particle velocity patterns at t = 3s for, a. TDP. b. RDP.

The time-averaged radial velocity of particles at different bed heights of 0.07, 0.105, and 0.14 meter for both cases were plotted in Figures-7 and 8. The existence of a symmetry core-annular region can be clearly observed in Figure-7. The particles velocity is minimum at the wall sides due to the high flow resistance to the walls and it increased to maximum values at the peaks where the wall resistance is negligible. The higher particles velocity can be observed in the annular region where particles fall down along the wall and it decreases up to the core region where the particles are carried up by the gas.

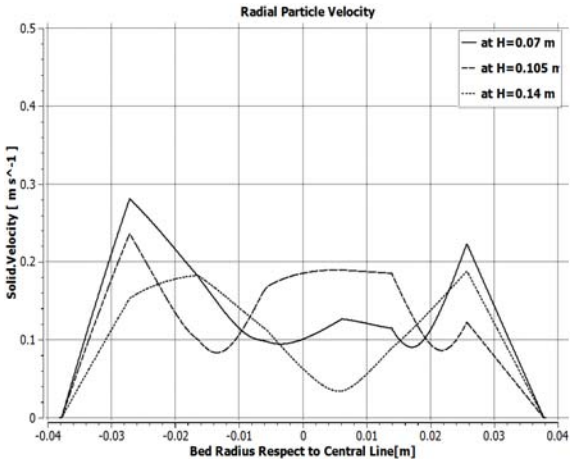

Figure-7. Time-averaged particle velocity profiles of TDP in the radial direction at t = 3s for three different bed heights of h = 0.07, 0.105 and 0.14 m.

On the contrary, Figure-8 shows different particle velocity trend. The core-annular region cannot be detected and the velocity pattern at different heights of the bed was changed significantly. For example, the change in the particle velocity at the height of 0.07 m is negligible. This can cause dead zones at the bottom of the bed. Besides, the high particle velocity at the bed surface (h=0.14 m) can be due to the falling particles thrown to the riser.

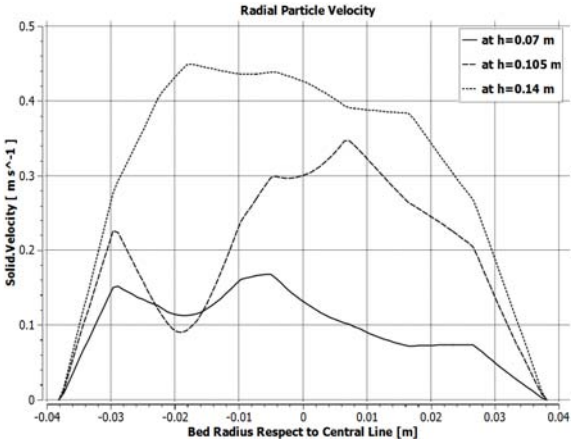

Figure-8. Time-averaged particle velocity profiles of RDP in the radial direction at t = 3s for three different bed heights of h = 0.07, 0.105 and 0.14 m.

Moreover, considering fluidized beds reactors, the feeders could be mounted at various heights above the gas distributor plate which is slightly above the bed surface. Therefore, in the case where fine particles are thrown up to this height, they would be gone into the feeders, creating operational hazards, and possible chocking of the feeder due to coking near its mouth. Since the values of particle velocity after bursting the bubbles on the surface of the bed for RDP is considerably higher than TDP, the possibility of the particles being thrown into the feeders would be increased. Hence, using the distributor plate having triangular pitch will somewhat solve this issue.

The axial pressure drop across the bed was plotted in Figure-9 for both cases. This is an important parameter in designing a gas distributor plate. In order to minimize the power consumption, a gas distributor plate needs to operate at a low pressure drop as possible. However, if it gives a too low pressure drop, poor fluidization would occur.

The graphs show the trend in the pressure drop which is generally decreased with increasing bed height. The reduction pattern is almost the same for both cases. However, the graph of RDP shows significant difference in the pressure drop in the region close to the distributor plate which could be due to the existence of the gas jet above the central hole. The TDP graph rises from 940 Pa at the distributor plate surface to a peak of 1060 Pa at the height of 0.019 m above the distributor plate. It then slopes down to the value of 580 Pa at the radial center of the bed. From this point, the downward trend continues falling sharply till it hits a zero value at 0.146 m. This significant pressure drop results from bubble movement.

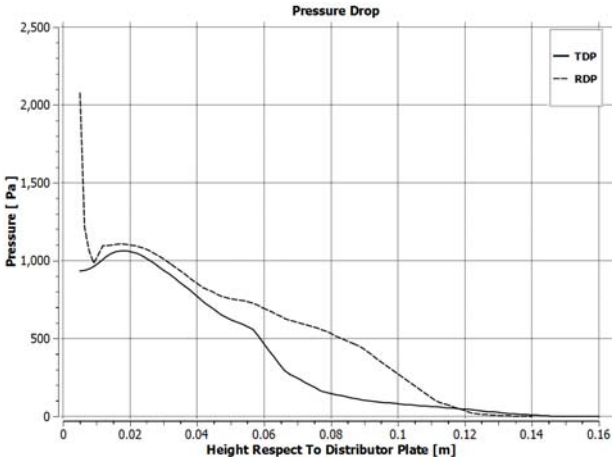

Figure-9. Comparison of axial pressure drop at t = 3s for both cases.

CONCLUSIONS

The lab-scale cold flow model was simulated using ANSYS Fluent 15. Comparing the simulation results, the chaotic motion of solid phase was observed for RDP. This is mainly affected by the nonuniform distribution of the bubble phase. Bubbles are mostly distributed in the region near the wall.

On the other hand, TDP shows more uniform particle distribution pattern. Bubbles are most appeared and rise in the central region of the bed caused uniform upward and downward motions of the particles in the core region and in the vicinity of wall, respectively. The uniform gas distribution pattern inside the bed is the main function of the gas distributor plate.

REFERENCES

[1] Basu P. 2006. Combustion and gasification in fluidized beds. Boca Raton: CRC/Taylor & Francis.

[2] Jackson R. 1963. The Mechanics of Fluidized Beds. Transactions of the Institution of Chemical Engineers. 41.

[3] SOO S. L. 1967. Fluid Dynamics of Multiphase System. Blaisdell, Waltham, MA.

[4] Garg S. K., and Pritchett J. W. 1975. Dynamics of Gas-Fluidized Beds. Journal of Applied Physics. 46,4493.

[5] Arastoopour H. and Gidaspow D. 1979. Analysis of IGT pneumatic conveying data and fast fluidization using a thermohydrodynamic model. Powder Technology. 22, 77.

[6] Gidaspow, D. and Ettehadieh B. 1983. Fluidization in Two-Dimensional Beds with a Jet. 2. Hydrodynamic Modeling. Industrial & Engineering Chemistry Fundamentals. 22,193.

[7] Ettehadieh B. Gidaspow D. and Lyczcowski R. W. 1984. Hydrodynamics of Fluidization in a Semicircular Bed with a Jet. AIChE Journal. 30, 529.

[8] Gidaspow D. 1986. Hydrodynamics of Fluidization and Heat Transfer: Supercomputer Modeling. Applied Mechanics Reviews. 39.

[9] Lyczkowsky R. W., Folga S., Chang S. L., Bouillard J. X., Wang C. S., Berry G. F. and Gidaspow D.1989. State-of-the-art computation of dynamics and erosion in fluidized bed tube banks. The Canadian Journal of Chemical Engineering. 67, 465.

[10] Eslami Afrooz I., Sinnathambi C. M., Karuppanan S. and Ling Chuan Ching D. 2015. Scaled down design of a cold and hot flow model based on a bubbling fluidized bed pilot plant gasifier. Applied Mechanics and Materials.

[11] Armstrong L. M., Gu S. and Luo K. H. 2010. Study of wall-to-bed heat transfer in a bubbling fluidised bed using the kinetic theory of granular flow. International Journal of Heat and Mass Transfer. 53, pp. 4949-4959.

[12] Altantzis C., Bates R. B., and Ghoniem, A. F. 2015. 3D Eulerian modeling of thin rectangular gas–solid fluidized beds: Estimation of the specularity coefficient and its effects on bubbling dynamics and circulation times. Powder Technology. 270, pp. 256-270.

[13] Li T., Zhang Y., Grace J. R., and Bi X. 2010. Numerical investigation of gas mixing in gas-solid fluidized beds. AIChE Journal. 56, pp. 2280-2296.

[14] Syamlal M., Rogers W., and O'Brien T. J.1993. MFIX documentation: Theory guide," National Energy Technology Laboratory, Department of Energy, Technical Note. DOE/METC-95/1013 and NTIS/DE95000031.

[15] Lun C. K. K., Savage S. B., Jeffrey D. J., and Chepurnity N. 1984. Kinetic theories for granular flow: inelastic particles in Couette flow and slightly inelastic particles in a general flow field. Journal of Fluid Mechanics, 140, pp. 223-256.

[16] Patankar S. 1980. Numerical heat transfer and fluid flow: CRC Press.